*36th EPS Conference on Plasma Phys. Sofia, June 29 - July 3, 2009 ECA Vol.**33E**, P-2.111 (2009)*

Microwave Air-Water Plasma Torch – Experiment and Theory

E. Felizardo[1], E. Tatarova[1], F.M. Dias[1], C.M. Ferreira[1] and B. Gordiets[2]

[1] *Instituto de Plasmas e Fusão Nuclear, Instituto Superior Técnico, Lisbon, Portugal*

[2] *Lebedev Physical Institute of the Russian Academy of Sciences, Moscow, Russia*

In the present work, an experimental and theoretical investigation of a surface wave sustained, microwave air-water plasma torch at atmospheric pressure is presented. Non-intrusive emission spectroscopy techniques have been used to map the rotational (gas) temperature, and the emission intensities of radiative species along the surface wave generated plasma torch. Some of the experimental data is validated by a comparison with the results of a 1D theoretical model based on a self-consistent treatment of particles kinetics, gas dynamics and wave electrodynamics.

The surface wave induced microwave plasma torch is created using a waveguide surfatron [1] based setup (Fig. 1). Microwave power is provided by a 2.45 GHz generator (Sairem) at levels varying from 200 to 700 W. The generator is connected to a waveguide (WR-340) system, which includes a circulator, a 3-stub tuner and a waveguide surfatron as the field applicator. The system is terminated by a movable short-circuit allowing maximization of the electric field at the launcher position. The discharge takes place inside a quartz tube with internal and external radii of 7.5 and 9 mm, respectively, inserted perpendicularly to the widest wall of the waveguide. Air is mixed with water vapour in a temperature-controlled environment and the mixture is driven into the discharge along heated metallic tubes to avoid condensation. The total gas flow ranges from 100 to 2000 sccm. Light emitted by the discharge is collected perpendicularly to the discharge tube by an optical fibre and conducted to the entrance of a Jobin-Yvon Spex 1250 spectrometer equipped with a nitrogen-cooled CCD camera. The plasma emission in the 250 nm - 850 nm range has been investigated as a function of the axial position and the microwave power.

The input parameters for the theoretical model are: pressure (760 torr); initial gas composition, i.e., air and water vapour; inner radius R, and wall thickness ΔR; dielectric permittivity, $_d$, of the tube; supplied microwave power P; microwave frequency, ; gas flow rate, Q; and wall temperature along the tube. The system of equations considered to describe the plasma source includes:

i) Maxwell's equations;

ii) the dispersion equation for the azimuthally symmetric TM surface mode;

iii) the rate balance equations for vibrationally excited states of electronic ground state molecules N_2 ($X^1\Sigma_g^+$,);

iv) the rate balance equations for the excited states of molecules and atoms $N_2(A)$, $N_2(B)$, $N_2(a')$, $N_2(a)$, $N_2(C)$, $N_2(a'')$, $N(^2D)$, $N(^2P)$, $O_2(a)$, $O_2(b)$, $O(^1D)$, $O(^1S)$;

v) the rate balance equations for electrons and the ions N_2^+, N_4^+, O^+, O_2^+, O_4^+, NO^+, NO_2^+, H_2O^+, H_3O^+, H_2^+, H_3^+, HN_2^+, NH_3^+, NH_4^+, O^-, O_2^-, O_3^-, H^-, OH^-, NO_2^-, NO_3^-;

vi) the rate balance equation for ground state molecules and atoms N, O, O_3, NO, N_2O, NO_2, NO_3, N_2O_5, H_2O, H, H_2, OH, HO_2, H_2O_2, NH_3, NH_2, NH, HNO, HNO_2, HNO_3;

vii) the gas thermal balance equation;

viii) the equation of mass conservation for the fluid as a whole.

A number of chemical and physical processes described in detail in [2] have also been taken into account.

The rotational temperatures of the OH radical (0-0 band of the $A^2\Sigma^+$-$X^2\Pi$ transition) have been determined by comparing the detected spectra with calculated ones [3]. A typical spectrum of the Q_1 branch of the observed OH (0-0) band at different percentages of water vapour is shown in Fig. 2.

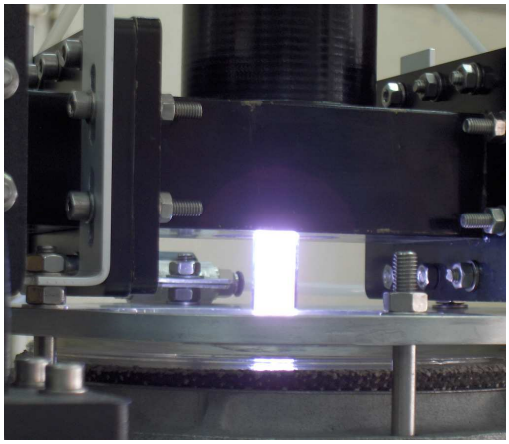

Fig. 1. Air-Water plasma torch

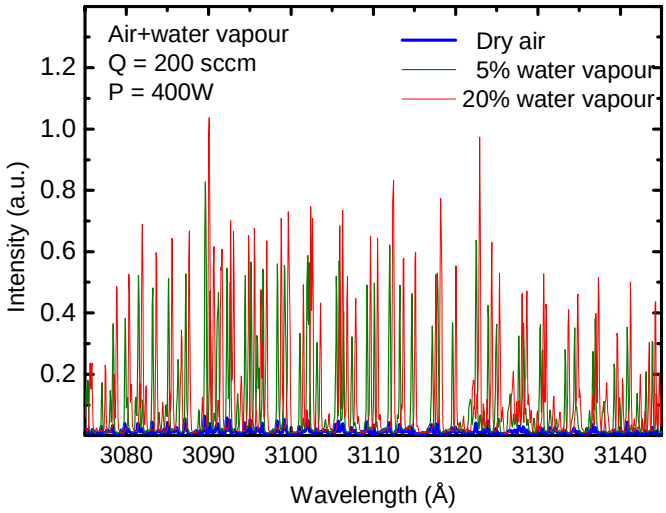

Fig. 2. OH spectra for three different percentages of water vapour.

The gas temperature in the discharge zone is a smooth function of the total microwave power delivered to the launcher for a fixed axial position as seen in Fig. 3. Note that the increase/decrease of absorbed power per unit volume leads to an increase/decrease of the gas temperature. However, it causes a growth/decrease of the electron density and, consequently, a decrease/increase of the local wave attenuation coefficient. In this way, the changes in the gas temperature at fixed axial position are somewhat restricted when the total delivered power

changes and there is no significant variation when the percentage of water vapour is changed up to 20 %, as seen in Fig. 4.

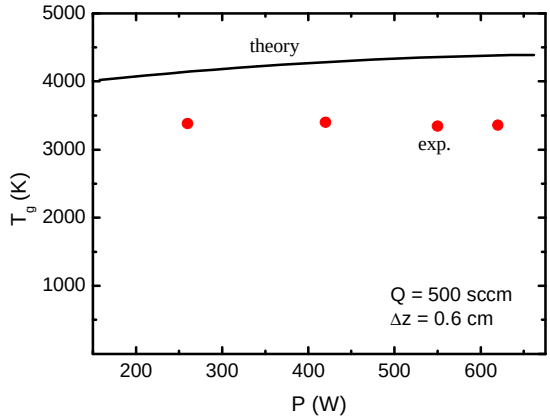

Fig.3. Dependence of the gas temperature on the microwave power delivered to the launcher (1% water vapour).

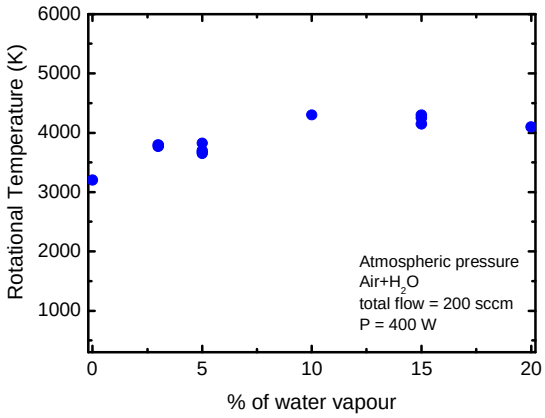

Fig. 4. Gas temperature vs the percentage of water vapour.

Small changes in the UV radiation of the NO(γ) band in the range 230-260 nm with the percentage of water vapour have been detected (see Fig. 5). However, a significant increase in the OH emission has been observed when the percentage of water vapour increases up to 10% in the mixture as seen in Fig. 6.

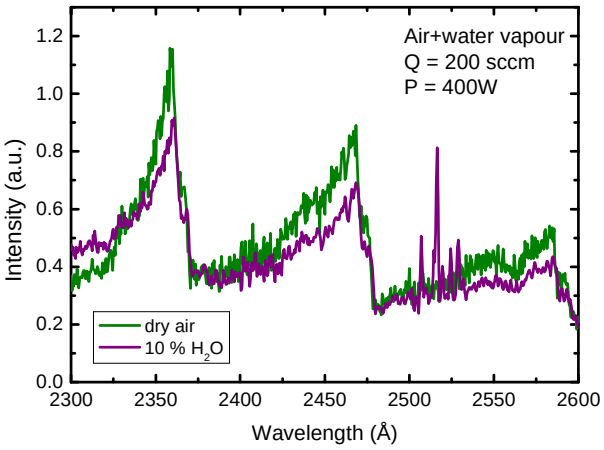

Fig. 5 NO( ) spectra for different percentages of water vapour.

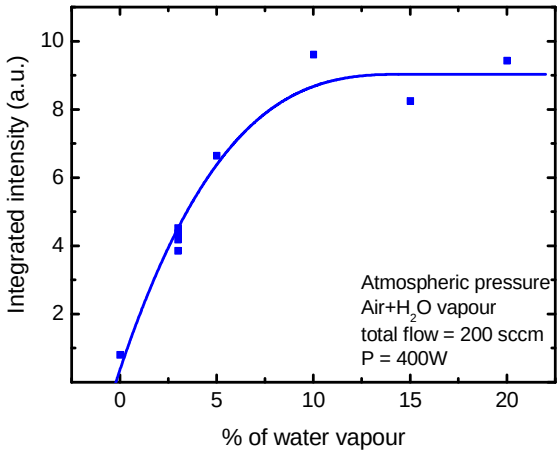

Fig. 6. OH integral intensity *vs.* percentage of water vapour.

The intensity of the NO(γ) band decreases in a relatively smooth way along the main part of the discharge and is followed by a sharp drop in the post-discharge zone of the plasma torch (Fig. 7).

The variation of the surface wave attenuation coefficient along the plasma column is shown in Fig. 8, as obtained by numerical differentiation of the wave amplitude records.

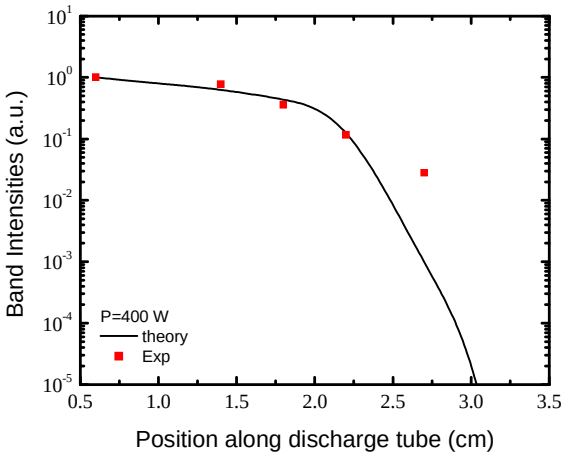

Fig. 7. Axial dependence of the intensity of NO( ) band radiation. Points – experiment; curve – model calculations (1% water vapour).

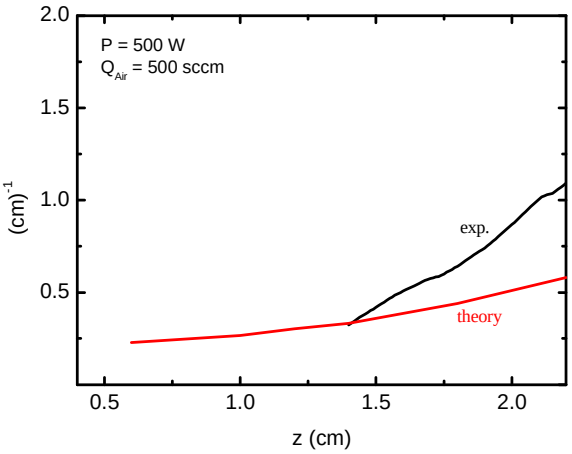

Fig. 8. Attenuation coefficient axial dependence

The gradual increase of the wave attenuation along the major part of the column is followed by a sharp rise close to the end, as both the theoretical and experimental results demonstrate [4]. This is a consequence of the simultaneous decrease in electron density and increase in electron-neutral collision frequency towards the column end (under the nearly isobaric conditions of the present experiment).

Acknowledgements

We would like to thank the financial support of the Foundation for Science and Technology, Portugal.

References

[1] M. Moisan, M, Chaker, Z. Zakrzewski e J. Parasczak, J. Phys. E: Sci Instrum. **20**, (1987) 1356.

[2] M. Capitelli, C.M. Ferreira, B.F. Gordiets and A.I. Osipov, "Plasma Kinetics in Atmospheric Gases", Springer, Berlin, Heidelberg, N.-Y., London, Paris, 2000.

[3] LIFBASE, Database and Spectral Simulation for diatomic molecules (v 1.6) – J. Luque e D.R. Crosley, SRI International Report MP-99-009 (1999).

[4] B. Gordiets, M. Pinheiro, E. Tatarova, F.M. Dias, C.M. Ferreira and A. Ricard, Plasma Sources and Sci. Technol., **9**, pp. 295-303, 2000.